Real-Time Experimental Control in Cellular Neurophysiology

A. D. Dorval, T. I. Netoff, J. A. White
Department of Biomedical Engineering and Center for BioDynamics,
Boston University, Boston, MA, USA

Abstract – **Electrophysiologists study neuronal input-output behavior by approximating synaptic input with a predetermined current waveform. In living tissue however, a synaptic event induces a conductance change in the neuronal membrane, and the current passed through that conductance is not predetermined, but a function of the continuously changing membrane potential. Using high frequency feedback, the dynamic clamp technique allows experimentalists to introduce conductance changes in living neurons. Using dynamic clamp, we find that current steps elicit greater membrane potential variance than more natural conductance steps. In addition, reliability profiles to the same pseudo-synaptic waveform change when currents are substituted for conductances. Hence, under certain conditions current input is an invalid approximation of conductance changes, and dynamic clamp should be used to examine neuronal input-output behaviors. Furthermore, dynamic clamp can be used as a control tool for other neuronal experiments. We demonstrate the use of a dynamic clamp as a signal detector, a frequency control device, and as a way to connect living cells to virtual networks. Thus we show that the dynamic clamp technique is a critical tool not only useful for mapping neuronal input-output function, but in a broader context of neuronal control.**

Keywords – **response curve, noise, spike-time variability**

I. Introduction

Neural activity is founded upon the ability of individual neurons to process input received from their neighbors. Quantifying how neurons process their input requires mapping neuronal output as a function of the signals a cell may be exposed to *in vivo*. The vast majority of neurons receive signals as chemical- or voltage-induced, synaptic conductance inputs. They process information with various intrinsic conductances, and generate outputs (i.e. action potentials) via quick and massive conductance changes. Typically, an electrophysiologist uses the current clamp technique to stimulate a neuron. In this method, a current waveform is provided to a cell, and the subsequent membrane potential recorded and analyzed. While useful for simple characterizations, this method lacks the ability to accurately describe behavior as a function of conductance changes, the native neuronal input modality.

Introduced in the past decade, the dynamic clamp technique can be used to examine how cells respond to conductance changes, by providing conductance waveforms to neurons [1,2]. This tool for exploring neuronal input-output function works in three steps. First, a cell's membrane voltage is measured. Second, a current is calculated as a function of the desired conductance waveform and the membrane voltage. Third, that calculated current is passed to the neuron. For dynamic clamps to simulate realistic conductances, currents must be calculated and fed back on the shortest time-scale relevant to a neuron: on the order of tens of microseconds. Difficult to achieve a decade ago, exponential growth in computer speed has recently enabled such high frequency feedback [3].

We use the dynamic clamp to examine input-output function in stellate cells of the medial entorhinal cortex (MEC). In these neurons, we study how cellular outputs are different under applied current conditions than under applied conductance conditions. We perform two sets of experiments. First, we examine subthreshold membrane statistics induced by constant current or conductance. Second, we quantify cell reliability to an input waveform similar to the synaptic bombardment that a cell would receive *in vivo*, applied as a current or a conductance.

Dynamic clamp can be used to perform feedback tasks beyond simple conductance calculations. We demonstrate a dynamic clamp simultaneously serving as: a signal detection device; a frequency control system; and as a pair of complementary synapses that couple a living neuron to an entirely computational cell, which is also being simulated by the dynamic clamp computer. In this experiment, we explore the extension of spike time response curve (STRC) methods to electrophysiology [4,5].

II. Methods

Horizontal sections comprising of the MEC and the hippocampus were prepared from 12 to 22 day old Long-Evans rats, according to approved protocols. Briefly, animals were anesthetized with carbon dioxide, and decapitated. Horizontal brain slices (350μm) were cut, transferred to an artificial cerebral-spinal fluid (ACSF) chamber, and allowed to incubate for over an hour.

Slices were submerged in 34º C, oxygenated ACSF, under an infrared differential interference contrast equipped microscope. Pipettes of 4 to 6 MΩ were patched onto visualized stellate cells. An electrode within the pipette was connected via a current clamp amplifier to a personal computer running a dynamic clamp program.

The dynamic clamp sampled the neuronal membrane potential (V_m), and calculated a current (I_{app}) to be provided. The dynamic clamp supplied a control signal to the amplifier which passed a corresponding current to the neuron. The dynamic clamp system injected either predetermined current waveforms $\{I_{app} = f(t)\}$, or feedback required conductance waveforms $\{I_{app} = f(V_m,t)\}$.

In the simple feedback case, the current was found as $\{I_{app} = G_{app}*[V_{rev}-V_m]\}$, where V_{rev} was set to 0mV, the

Support for this work was provided by the National Institute of Health, R29-NS34425, and by the National Science Foundation, BES-0085177.

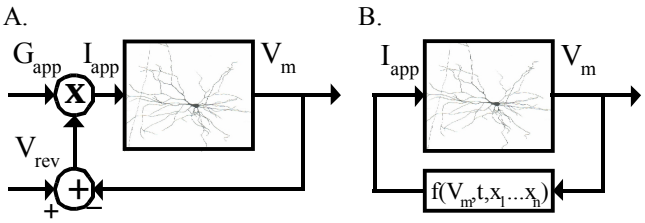

Figure 1. Schematic diagram of a dynamic clamp experiment. Membrane potential, V_m, is used to calculate the current injected into the neuron, I_{app}. Stellate cell drawing courtesy of Julie Haas. (A.) Traditionally, dynamic clamps find I_{app} as the product of an applied conductance, G_{app}, and the difference between a reversal potential, V_{rev}, and V_m. (B.) In a broader context, I_{app} can be a generic function, f, of V_m, time, and a number of input values, x_i. This reduces to the original model when, $f = G_{app} * [V_{rev} - V_m]$.

typical reversal potential of an excitatory synapse, and G_{app} was the conductance (Fig. 1A). In the first set of experiments, G_{app} was held constant, and in the second it was a time varying, frozen-noise signal.

More complex feedback was required for the third set of experiments (Fig. 1B). These were designed around STRCs, which describe how small inputs affect cell firing time [4]. STRC methods treat neurons as periodic oscillators whose frequency is the neuronal firing rate. When a small perturbation is delivered to a neuron, the next spike time will be slightly advanced or delayed from its normal firing time. By providing small inputs at all phases of the inter-spike interval, a map can be constructed that describes when the next spike time will occur, given the phase at which the perturbation is delivered. This map is the STRC.

In phase one of the these STRC experiments, the dynamic clamp detected spike times. A control algorithm in the dynamic clamp raised or lowered a direct current to keep inter-spike intervals at 150ms, ensuring that cells behaved as periodic oscillators. The dynamic clamp presented small perturbations (synaptic-like conductance changes) to the cell, and mapped the time advance (or delay) of the next spike. In phase two of the experiment, the dynamic clamp simulated a neuron from the STRC, and bidirectionally coupled it to the cell via virtual synapses [5].

III. Results

The first set of experiments explored how neuronal response was differentially affected by conductance and current steps. Depolarizing input steps of both current and conductance, at amplitudes below that required to elicit stellate cell firing, were generated via dynamic clamp (Fig. 2A). In the conductance condition, the applied current, I_{app}, was calculated as described in methods, from a constant applied conductance. In the current condition, I_{app} was held constant. Conductance and current steps were interlaced, with varying amplitudes presented in random order.

Membrane potential statistics were examined for the two input types. For direct comparisons, current trials were matched with conductance trials of similar applied current. Whether the input was a current or a conductance did not

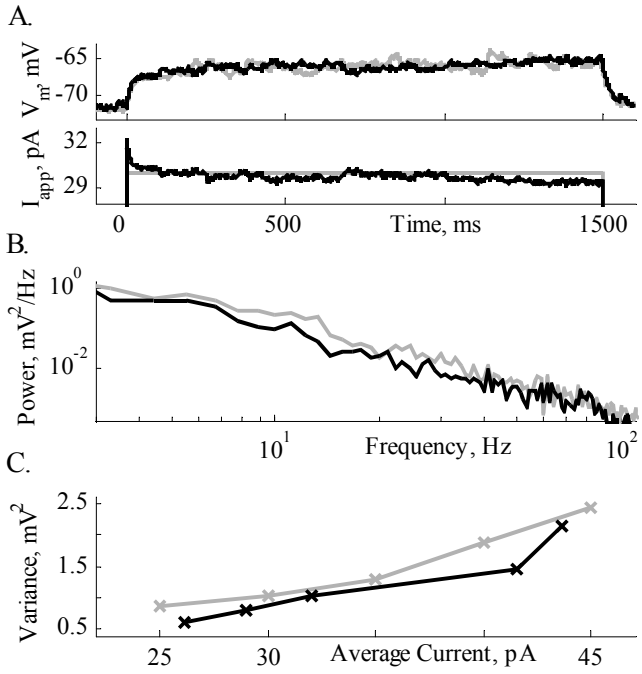

Figure 2. Membrane potentials were examined in response to either current or conductance. Conductance condition data are shown in black; current condition data in gray. (A.) Two example data traces. *Bottom* – Applied current, I_{app}, as a function of time, rising from 0pA at t=0. Note that I_{app} is not constant for the conductance condition. *Top* – Resulting membrane potentials, V_m. (B.) Averaged power spectra for ten current and ten conductance trials of approximately equal average I_{app}. (C.) Membrane potential variances plotted as a function of average I_{app}.

affect average membrane potential, but it did play a role in setting higher order statistics. While the average applied current of a conductance trial never precisely matched the I_{app} of a current trial, power spectra were contrasted between trials of approximately equal I_{app} (Fig. 2B). These power spectra suggest that current steps yielded more energy at frequencies below 40Hz than conductance steps. Membrane potential variance was calculated for both modalities over a range of input amplitudes (Fig. 2C). The results show that constant current elicits a noisier membrane potential than constant conductance.

The second set of experiments was designed to examine how reliably physiologically realistic levels of noisy input are converted into spike trains [6], and how accurately synaptic current events can substitute for synaptic conductance events. Roughly, the procedure described above was repeated with frozen-noise waveforms as replacements for the simple current and conductance steps (Fig. 3A, bottom). The frozen-noise was constructed in real-time, to resemble synaptic bombardment *in vivo*. It consisted of a 200Hz Poisson pulse train convolved with the function $\{t * \exp(-t/\tau)\}$, where τ was set to 5ms. Each frozen-noise waveform was presented to the cell ten times in both modalities, and at several amplitudes.

Rastergrams, showing all spike times in a given trial, were constructed for each trial. Reliability profiles were calculated the following way. A unit-height Gaussian

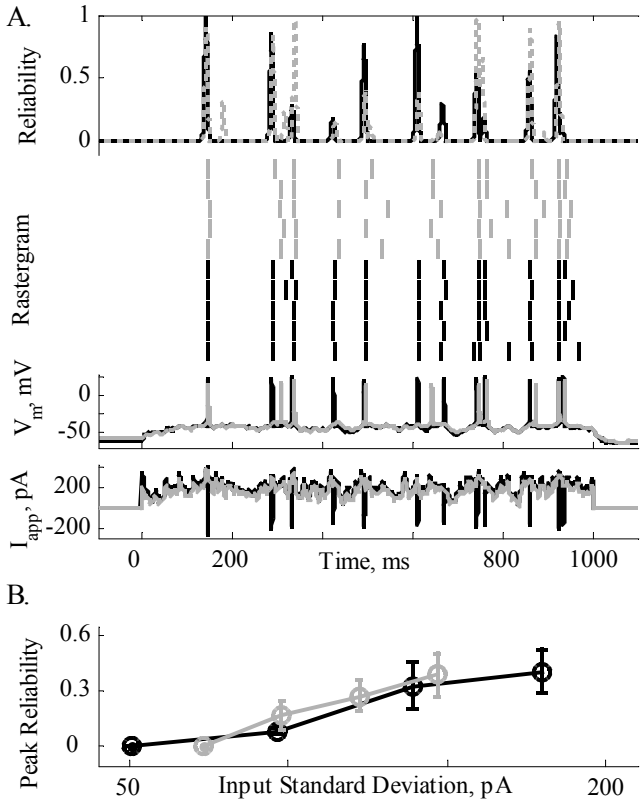

Figure 3. Spike time reliabilities were examined in response to pseudo-synaptic bombardment presented as either current or conductance. Conductance condition data is shown in black; current condition data in gray. (A.) Example data traces. *Bottom* – As in Fig. 2, applied current traces, I_{app}, are shown beneath the membrane potentials they induce. Note that the current traces are similar except for the large deviations coincident with membrane potential spikes. *Middle* – Each input was repeated multiple times. Rastergrams, which show when spikes occur, were found for every trial and both input conditions. *Top* – As described in the results, reliability profiles were found for each input type. (B.) Peak reliability distributions were found from reliability profiles. Plotted against the standard deviation of the applied current, this measure appears independent of input modality.

function of 3ms standard deviation was convolved with each rastergram. Reliabilities for each spike were calculated as the average value of the other nine convolved rastergrams from the same stimulus type, at the time of the individual spike in question. The rastergrams from like trials were averaged, each spike scaled by its reliability, and that waveform convolved with the same Gaussian function to yield reliability profiles (Fig. 3A, top). These profiles range from near zero when no more than one spike occurred in a ~10ms window in any trial, to a value of one when a spike occurred at the exact same moment in all ten trials.

The reliability profiles indicate that some pseudo-synaptic events elicited spikes more reliably than others, and that current and conductance inputs were not treated equally. Some conductance events caused very reliable spikes while their current equivalents did not, and vice-versa. The distributions of reliability peaks were examined for a range of input variances (Fig. 3B). Not surprisingly, larger input variances corresponded to higher peak reliabilities for both

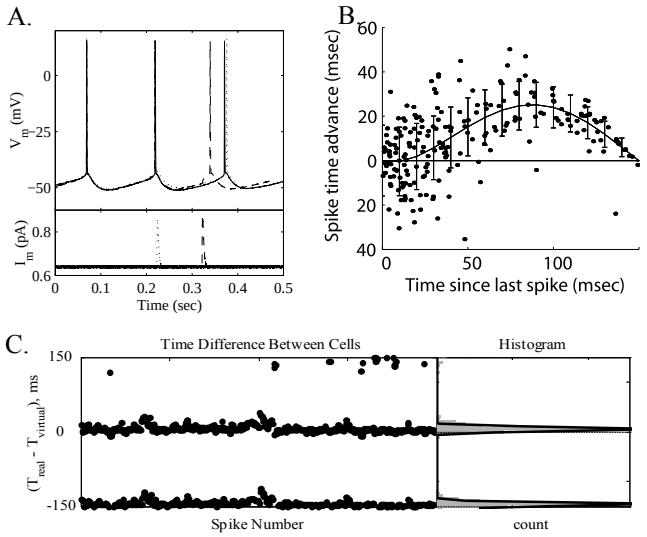

Figure 4. STRCs were measured and used to create a two-cell hybrid network that consisted of one real and one virtual neuron. (A.) Example data traces. A control current was injected to keep the cell firing at a rate of 6.6Hz. *Bottom* – Synaptic conductance events were presented at random times. *Top* – The solid line shows the voltage waveform in the absence of synaptic events. One event advanced the time of the next spike, dashed, while the other delayed the time of the next spike, dotted. (B.) The elicited advance or delay was plotted against the arrival time of the synaptic event. STRCs were calculated as polynomial fits to the mean and variance of the resulting scatter plot. (C.) A virtual neuron was constructed and coupled to the real cell, as described in the text. *Left* – The spike time difference between the two cells over many trials. A difference of any integer multiple of 150ms amounts to synchronous firing. *Right* – Shown in gray is the histogram of the spike time differences. The cells usually fired within a few milliseconds of each other. The black line is a prediction from a purely computational network of two such virtual cells.

input types. There were not however, any discernible differences in the average reliabilities between the current and conductance modalities.

A final set of experiments was conducted to study the viability of experimental spike time response methods [4,5], given the various ways in which noise may prohibit the construction of clean STRCs. The dynamic clamp was used to maintain stellate cell firing rate at 6.6Hz. At random times, the dynamic clamp also provided excitatory pseudo-synaptic conductances to the neurons (Fig. 4A), and measured the time of the next spike. The difference between each actual spike time and the time predicted from the 6.6Hz firing rate was plotted as a function of the time difference between the previous spike and the pseudo-synaptic event (Fig. 4B). STRCs were generated as polynomial fits to the data, with a value of variance that depended on spike timing.

The dynamic clamp and STRC were then used to create a hybrid network, whereby a virtual neuron was bidirectionally coupled to the living cell. As described above, the dynamic clamp held the firing rate of the living neuron at 6.6Hz. Every time the virtual cell spiked, a pseudo-synaptic conductance was passed to the living cell. Virtual cell spike times were determined as follows. The virtual cell was constructed to fire at roughly 6.6Hz, and the first firing time was chosen at random. The time-since-last-

spike was measured as the time between the first virtual cell spike and the following real cell spike. A virtual spike-time-advance was found by passing the time-since-last-spike through the fitted STRC (Fig. 4B). The next virtual spike time was calculated as 150ms after the previous virtual spike time, minus the spike-time-advance.

This method to calculate the virtual spike time was repeated for the second virtual spike, and the third, and so on. The two cells quickly settled into a synchronous firing pattern where they usually fired at about the same time for hundreds of cycles (Fig. 4C). Variability in spike times occasionally drove the system out of synchrony, but these deviations were short lived. Histograms representing measured spike time differences were essentially identical to results predicted from the STRC.

IV. Discussion

In the subthreshold regime, a stellate cell's average membrane potential is a simple function of average applied current, regardless of whether that current is calculated from a conductance or applied directly. Perhaps surprisingly, the same cannot be said of membrane potential variance. Conductance inputs lead to a less variable voltage waveform. This can be understood by considering the applied current equation, $\{I_{app}=G_{app}*[V_{rev}-V_m]\}$. Assuming V_m is at rest, a small depolarization of V_m will reduce I_{app}, thus driving V_m back to its rest value; a hyper-polarization will increase I_{app}, also driving V_m back to rest. In contrast, a slight change of V_m under current step conditions will not affect I_{app}, and the noisy dynamics of the cell will be left to drive the membrane potential along its circuitous path.

In response to synaptic barrages of either current or conductance, stellate cells respond equally reliably. This result is difficult to reconcile with the distinction that stellate cells seem to draw between reliable current events, and reliable conductance events. More work needs to be done in this direction, to further explore the validity of the synaptic current clamp barrage approximation.

Along with others, we are exploring the ways that spike time response methods can simplify neural analysis. As expected, experimental STRC are notably noisy, particularly when compared to their theoretical counterparts. With an experimentally collected STRC however, two-cell hybrid network behavior can be accurately predicted via purely computational simulations. This suggests that spike time response methods have a bright future, if ways can be found to incorporate realistic noisy distributions into the existing theoretical framework.

Dynamic clamp systems are quickly becoming a required tool for the technologically savvy. Envisioned to create neuronal inputs in a more natural way, a fast and powerful dynamic clamp should now be viewed as a neuron control system that can be used to probe cells in countless novel ways. In a single experiment we used a dynamic clamp for three purposes beyond simple current and conductance injection. First, as a signal detection device, it precisely determined when spikes occurred. Second, as a frequency control device, it maintained a constant firing rate by adjusting applied current to the cell. Third, as a virtual network, it simulated a second cell, and coupled it to the living neuron.

V. Conclusion

Neurons respond to current and conductance inputs differently. While average reliability is the same, neurons select for different features within current and conductance waveforms. Since conductance changes are the natural input to neurons, dynamic clamp should replace current clamp as the standard technique for examining neuronal input-output function. Dynamic clamp can also be used to explore neuronal behavior in novel experiments that go beyond simple conductance clamp, such as our STRC experiments. To explore these possibilities, we encourage you to download our open source dynamic clamp [3], which runs on either the RTLinux or the RTAI-Linux operating systems: www.bu.edu/bme/ndl/rtldc.html .

References

[1] Robinson H.P.C., Kawai N. “Injection of digitally synthesized synaptic conductance transients to measure the integrative properties of neurons.” J. Neurosci. Methods, 49:157-165, 1993.

[2] Sharp A.A., O'Neil M.B., Abbott L.F., Marder E. “The dynamic clamp: artificial conductances in biological neurons.” Trends Neurosci., 16:389-394, 1993.

[3] Dorval A.D., Christini D.J., White J.A. “Real-time linux dynamic clamp: a fast and flexible way to construct virtual ion channels in living cells.” Ann. Biomed. Eng., 29:897-907, 2001.

[4] Ermentrout B. “Type I membranes, phase resetting curves, and synchrony.” Neural Comp., 8:979-1001, 1996.

[5] Acker C. D. “Synchronization of strongly coupled excitatory neurons: relating biophysics to network behavior.” M.S. Thesis, Boston University, Dept. of Biomedical Engineering, 2000.

[6] Mainen Z. F., Sejnowski T. J. “Reliability of spike timing in neocortical neurons.” Science, 268:1503-1506, 1995.